Temperature, by controlling growth rate, regulates CRISPR-Cas activity in *Pseudomonas aeruginosa*

Nina Molin Høyland-Kroghsbo[a], Katrina Arcelia Muñoz[a*], Bonnie L. Bassler[ab]#

[a]Department of Molecular Biology, Princeton University, Princeton, New Jersey, USA

[b]Howard Hughes Medical Institute, Chevy Chase, Maryland, USA

Running head: Slow growth promotes CRISPR adaptation

#Address correspondence to Bonnie L. Bassler, bbassler@princeton.edu

*Present address: Bates College, Lewiston, Maine, USA.

Word count abstract: 165

Word count text: 5,299

Abstract

CRISPR-Cas (Clustered Regularly Interspaced Short Palindromic Repeats - CRISPR Associated) are adaptive defense systems that protect bacteria and Archaea from invading genetic elements. In *Pseudomonas aeruginosa*, quorum sensing (QS) induces the CRISPR-Cas defense system at high cell density when the risk of bacteriophage infection is high. Here, we show that another cue, temperature, modulates *P. aeruginosa* CRISPR-Cas. Increased CRISPR adaptation occurs at environmental (i.e., low) temperatures compared to body (i.e., high) temperature. This increase is a consequence of accumulation of CRISPR-Cas complexes, coupled with reduced *P. aeruginosa* growth rate at the lower temperature, the latter of which provides additional time prior to cell division for CRISPR-Cas to patrol the cell and successfully eliminate and/or acquire immunity to foreign DNA. Analyses of a QS mutant and synthetic QS compounds show that the QS and temperature cues act synergistically. The diversity and level of phage encountered by *P. aeruginosa* in the environment exceeds that in the human body, presumably warranting increased reliance on CRISPR-Cas at environmental temperatures.

Importance

P. aeruginosa is a soil dwelling bacterium, a plant pathogen, and it also causes life threatening infections in humans. Thus, *P. aeruginosa* thrives in diverse environments and over a broad range of temperatures. Some *P. aeruginosa* strains rely on the adaptive immune system CRISPR-Cas as a phage defense mechanism. Our discovery that low temperatures increase CRISPR adaptation suggests that

35 the rarely occurring but crucial naïve adaptation events may take place predominantly under
36 conditions of slow growth, e.g. during the bacterium's soil dwelling existence.

37

38 **Introduction**

39 Bacteria have evolved defense systems to fend off bacteriophage viruses that prey upon them.
40 One of these systems, CRISPR-Cas, provides acquired and heritable sequence-specific immunity
41 against previously encountered viruses and plasmids (1, 2). CRISPR-Cas systems generally rely on
42 three main activities; adaptation, expression, and interference (3). Upon infection with a foreign
43 genetic element, the CRISPR-Cas machinery can incorporate a short piece of foreign DNA into the
44 genomic CRISPR array, which contains the genetic memory of prior infecting elements. The CRISPR
45 array thereby expands in size by gaining an additional repeat and a spacer derived from the foreign
46 DNA. This process is known as adaptation (1, 4, 5). Next, during the expression stage, the CRISPR array
47 is transcribed into pre-crRNAs that are processed into mature crRNAs, each complementary to a
48 particular foreign DNA sequence. crRNAs guide Cas protein complexes to target complementary
49 incoming foreign DNA, denoted protospacers (6). Most CRISPR-Cas systems require the presence of a
50 short protospacer adjacent motif (PAM) to correctly identify the target DNA and distinguish it from
51 self (7, 8). The final stage is interference, when Cas immune surveillance complexes, guided by mature
52 crRNAs, cleave, and thereby, eliminate complementary foreign genetic material (9).

53 Naïve CRISPR-adaptation to a foreign genetic element that a bacterium has not previously
54 encountered is rare in type I CRISPR-Cas systems (10). However, when a crRNA has partial

55 complementarity to a protospacer sequence, the frequency of new spacer acquisition is enhanced
56 more than 500-fold (11). This process is known as primed adaptation (5). Primed adaptation is crucial
57 for type I CRISPR-Cas systems to robustly fight off contemporary threats, notably, when the foreign
58 element mutates, which would otherwise allow escape from CRISPR targeting (10). In this same vein,
59 CRISPR arrays possessing multiple spacers targeting the same phage reduce the chances that a phage
60 can acquire mutations that enable it to escape detection (12). This arrangement, moreover, allows a
61 larger proportion of CRISPR-Cas complexes to be loaded with crRNAs that target a particular infecting
62 phage, providing a more favorable CRISPR-Cas complex:phage target ratio, again increasing the
63 success of the defense system.

64 Naïve adaptation requires cleavage of the newly infecting DNA, incorporation of a short
65 fragment as a new spacer in the CRISPR array, transcription and processing of the new crRNA, and
66 formation of a crRNA-Cas complex to scan the genomic and foreign DNA to pinpoint the foreign DNA
67 and target it for cleavage. These steps take time. During that time, the phage is executing its parasitic
68 program, either lysogenizing the host, in which case adaptation would lead to host suicide, or
69 alternatively, generating numerous copies of the phage genome as the phage prepares to lyse the
70 host cell. With respect to the phage lysis program, it could be difficult for the CRISPR-Cas machinery
71 to keep pace - degrading phage genomes as new phage genomes are produced - possibly a
72 contributing feature underpinning why naïve adaptation is so infrequent. Indeed, in line with this
73 argument, defective phage particles capable of infecting but not killing host bacteria have been
74 shown to increase adaptation frequency (13). In this case, a defective phage injects its DNA, which can

75 serve as a substrate for naïve adaptation, in a setting in which the race between host killing and
76 CRISPR-Cas success does not occur.

77 Bacteria incorporate cues, such as nutrient availability into regulation of CRISPR-Cas (14-17).
78 We previously discovered that the cue for cell population density is integrated into CRISPR-Cas
79 regulation. Specifically, cell-cell communication, i.e., quorum sensing (QS), activates type I-F CRISPR-
80 *cas* expression, CRISPR-Cas activity, and CRISPR adaptation in *P. aeruginosa* UCBPP-PA14 (hereafter
81 denoted PA14), enabling CRISPR-Cas function to increase in step with increasing bacterial cell density
82 (18). This mechanism ensures maximum CRISPR-Cas activity when bacterial populations are at high
83 cell density and at highest risk for phage infection and spread. Likewise, Patterson *et al*. showed that
84 in *Serratia* sp. ATCC39006, the QS autoinducer synthase SmaI is required for expression and activity of
85 type I-E, I-F, and III-A CRISPR-Cas systems, as well as for adaptation of types I-E and I-F systems (19).
86 Together, these results suggest that QS regulation of CRISPR-Cas may be a general phenomenon
87 allowing bacteria to balance the risk of phage infection with the burden of producing CRISPR-Cas
88 complexes and the risk of suicide from autoimmunity.

89 Here, using mutagenesis and molecular analyses, we show that another cue, low temperature,
90 promotes CRISPR adaptation and interference in PA14. Specifically, at low temperature, CRISPR-Cas
91 complex levels increase and growth rate slows, each of which promotes increased adaptation. Using a
92 QS mutant and synthetic QS compounds, we show that the temperature and QS inputs act
93 synergistically. We hypothesize that the low temperature- and QS-mediated increases in CRISPR-Cas
94 complex abundance elevate the number of possible adaptation/interference events. Furthermore, the

95 reduced growth rate causes an apparent increase in CRISPR-Cas activity by providing the time
96 required for the CRISPR-Cas machinery to carry out all of the required steps - adaptation, expression,
97 and interference - for successful defense against a foreign invading element, prior to cell division. If,
98 simultaneously, the slow growth conditions were unfavorable for phage propagation, it would give
99 the CRISPR-Cas system the chance to accomplish the adaptation program prior to the cell becoming
100 overwhelmed by replicating phage, making this mechanism particularly effective.

101

102 **Results**

103 **Temperature affects CRISPR adaptation.**

104 *P. aeruginosa* is an environmental bacterium and an opportunistic human pathogen that causes
105 nosocomial infections and chronic lung infections in patients with cystic fibrosis (CF) (20). PA14, the
106 strain used in the present studies, was isolated from a burn victim. PA14 is, additionally, pathogenic in
107 both plants and mice (21). PA14 has a type I-F CRISPR-Cas system, providing it with resistance to
108 phage (22, 23).

109 Naïve CRISPR adaptation to a phage that a bacterium has not encountered previously is rare in
110 laboratory analyses of type I CRISPR-Cas systems (10). Adaptation requires cleavage of the foreign
111 phage DNA, incorporation of a new spacer in the CRISPR array, transcription and processing into a
112 mature crRNA, crRNA-guided detection of the foreign complementary DNA by the newly made crRNA
113 in the Cas complex, and target cleavage by a Cas nuclease. Crucially, all of those steps must occur

114 prior to the cell being overwhelmed by replicating phage DNA. We wondered if slowing bacterial
115 growth could buy a bacterium more time for its CRISPR-Cas machinery to successfully adapt to and
116 eliminate a foreign genetic element. This mechanism may be particularly relevant in the case of
117 plasmids, which do not kill the host, and in the case of multiple phage infections of a single host cell,
118 where the spacers acquired from one phage can be used against other invading phages. With this
119 thought in mind, we were struck by the versatility of *P. aeruginosa* with respect to its ability to
120 successfully reside both in the soil/plants and in mammalian hosts. These niches vary dramatically in
121 many respects, notably for our present work, with regard to temperature and phage exposure (24,
122 25). We hypothesized that slow growth, as experienced by *P. aeruginosa* in the cooler temperatures
123 of the phage ridden soil or during plant infection, rather than the higher temperature experienced
124 during human infection, could provide a favorable locale for CRISPR adaptation events to occur.

125 To assess whether temperature influences CRISPR adaptation, we measured the ability of
126 PA14 to adapt to the plasmid pCR2SP1 seed, when grown at 37, 30, 23, and 15°C. The pCR2SP1 seed
127 plasmid harbors a protospacer targeted by CRISPR2 spacer 1. The protospacer possesses a single base
128 mutation in the 5' seed region which fosters priming for CRISPR adaptation. During adaptation, new
129 CRISPR spacers are incorporated at the 5' end of a CRISPR array (1, 4). Thus, spacer number 1
130 becomes spacer number 2 and so on. This feature of the adaptation mechanism provides a
131 convenient means to track adaptation events by PCR amplification of the expanding region. In our
132 analysis, we used PCR primers flanking spacer number 1 of the CRISPR2 array. We separated the
133 products based on size and visualized the CRISPR spacer population. In PA14, introduction of each
134 new spacer and repeat adds 60 bp to the existing CRISPR array. In order to have minimal CRISPR-Cas

135 activity at the start of the experiment, cultures of PA14 were grown at 37°C to a low cell density, and
136 transformed with pCR2SP1 seed (18). Transformants were allowed to recover at 37°C for 1 h, and
137 subsequently, were grown on LB agar with gentamicin at the respective temperatures until they
138 reached 1 mm in diameter. Single colonies were analyzed for adaptation events by PCR. Fig. 1A shows
139 that PA14 cells grown at 37°C have a spacer population consisting primarily of the un-adapted parent
140 array with a minor subpopulation that gained one or two new spacers. Cas3, which cleaves DNA when
141 bound by the Csy1-4 complex, is required for adaptation to occur. Adaptation to the pCR2SP1 seed
142 plasmid appears to favor acquisition of two additional spacers rather than one or three additional
143 spacers. Often, an adaptation ladder is observed in which each new/additional adaptation event is
144 less frequent than the previous one, however, in the case of adaptation primed by plasmids, others
145 have also shown adaptation patterns similar to those in Fig. 1A (11, 26). We sequenced the
146 introduced spacers from 10 individual adaptation events, and found that all new spacers were derived
147 from the priming plasmid at locations within ~1 kb of the protospacer (data not shown). Notably, for
148 each decrease in growth temperature to 30, 23, and 15°C, PA14 contains a higher proportion of
149 adapted arrays. Quantification of these adaptation events shows that approximately 16% of the
150 spacer population is adapted when grown at 37°C and this proportion increases to 61% for PA14
151 grown at 15°C (Fig. 1B). Moreover, the fraction of arrays that acquired multiple spacers also increases
152 with decreasing growth temperature. Arrays containing three new spacers cannot be detected in cells
153 grown at 37°C, whereas approximately 8% of the cells grown at 15°C have acquired three spacers.

154 We envision three possible mechanisms that could underlie the increase in CRISPR adaptation
155 that occurs at low growth temperatures: 1. The CRISPR-targeted plasmid is present at higher copy-

156 number at low temperatures than at high temperatures, fostering higher rates of priming, and hence,
157 an increase in potential adaptation events. 2. CRISPR-Cas complexes are more abundant at low
158 temperatures than at high temperatures, which, again, would increase the chances for adaptation. 3.
159 The reduced bacterial growth rate at low temperatures compared to high temperatures could provide
160 CRISPR-Cas complexes additional time to perform all of the steps necessary to achieve immunity and,
161 hence, enable higher numbers of adaptation events to occur prior to each cell division. Any
162 combination of these three mechanisms is also possible and could contribute to the connection
163 between low temperature and high CRISPR adaptation frequency.

164

165 **Temperature does not affect pHERD30T copy number.**

166 First, we examined the possibility that temperature affects the relative copy number of the
167 incoming plasmid. To do this, we measured, at different temperatures, the relative copy number of
168 pHERD30T, the empty high copy vector backbone for the pCR2SP1 seed plasmid (23). PA14 cells
169 carrying pHERD30T were grown at 37, 30, 23, and 15°C. The relative copy number of pHERD30T was
170 assayed by qPCR of total DNA using the chromosomal *rpoB* gene as the control. Fig 2. shows that
171 there is no effect of temperature on the relative copy number of pHERD30T.

172

173 **Temperature has only a modest effect on Csy4 abundance.**

174 We examined the second possibility, that the level of the CRIPSR-Cas machinery present in
175 cells is affected by temperature. We reasoned that temperature could affect transcription,
176 translation, and/or the stability of Cas proteins. No matter which mechanism, the outcome would be
177 a change in cellular concentration of CRISPR-Cas complexes. Thus, we assessed the relative
178 abundances of CRISPR-Cas complexes at the different temperatures using Csy4-3xFLAG as the proxy.
179 Csy4 is a component of the Csy1-4-crRNA CRISPR-Cas complex that binds to and targets foreign DNA
180 for cleavage (22). A cross streak assay was performed to verify that CRISPR-Cas-dependent resistance
181 to the CRISPR-targeted phage DMS3m^{vir} was not affected by fusion of the 3xFLAG tag to Csy4 (Fig. S1).
182 In contrast to a ΔCRISPR Δ*cas* mutant strain lacking both CRISPR arrays, *cas1*, *cas3*, and *csy1-4*, which
183 succumbed to DMS3m^{vir} phage infection, the PA14 strain carrying *csy4-3xflag* was resistant,
184 suggesting that the Csy4-3xFLAG protein is functional.

185 To test whether growth temperature affects Csy4 levels, we grew PA14 at 37, 30, 23, and 15°C
186 and measured the relative abundance of Csy4 by Western blotting. Fig. 3 shows that relative to a
187 control protein, RpoB, Csy4-3xFLAG levels increase slightly with decreasing temperature. Quantitation
188 shows that there is 1.2- to 1.4-fold more Csy4-3xFLAG present at temperatures below 37°C (Fig. 3). To
189 address the possibility that temperature affects Csy4-3xFLAG stability in our assay, we grew WT PA14
190 carrying Csy4-3xFLAG at 23°C to OD_{600} = 1. We treated the culture with gentamicin to arrest protein
191 synthesis, divided the culture into two aliquots, and we incubated one aliquot at 23°C and the other
192 at 37°C for two more hours. Csy4 levels remained constant at both temperatures (Fig. S2). Using this
193 assay, we cannot however exclude the possibility that there may be temperature-dependent
194 differences in the stability of CRISPR-Cas complexes, which could contribute to the temperature-

195 dependent regulation of CRISPR-mediated adaptation. We suggest that the enhanced CRIPSR-
196 mediated adaptation that occurs at low temperatures (Fig. 1) can be explained by differences in the
197 abundance of CRISPR-Cas machinery alone or, perhaps, in combination with slow growth, as
198 investigated in the next section.

199

200 **Growth rate affects CRISPR-Cas activity.**

201 We examined the final possibility, that growth rate contributes to the temperature-dependent
202 effects we observe on CRISPR adaptation in PA14. For this analysis, we assayed the elimination of a
203 plasmid rather than a phage because temperature affects CRISPR-Cas-independent phage-host
204 interactions, including phage adsorption rates, plaquing efficiency, the lysis versus lysogeny switch,
205 and the activity of restriction modification anti-phage defenses (23, 27-30). Indeed, as one example of
206 these complexities, we show in Fig. S3 that the rate of JBD44a phage adsorption to PA14 is increased
207 at 23°C compared to 37°C, irrespective of the presence/absence of CRISPR-Cas. This temperature-
208 mediated effect on adsorption may be explained by increased long-chain O-antigen decoration of the
209 cell surface that occurs at low temperatures. These O-antigen moieties play phage receptor roles (31,
210 32).

211 To measure the influence of growth rate on the ability of CRISPR-Cas to eradicate a foreign
212 genetic element, we assayed CRISPR-Cas effectiveness in eliminating the CRISPR-targeted plasmid
213 called pCR2SP1 (23) when PA14 was grown at different rates. This pHERD30T-derived plasmid

214 contains a protospacer targeted by CRISPR2 spacer 1 flanked by a PAM sequence that is required for
215 CRISPR interference (7).

216 To control bacterial growth rate, we varied aeration levels by shaking the cultures at either
217 250 RPM or at 150 RPM. We note that we did not use minimal versus rich growth medium to control
218 growth rate because, as noted above, nutrient availability affects the activity of CRISPR-Cas systems in
219 multiple bacterial species, including PA14 (14-17, 33). Rather, we grew the rapidly/slowly shaken
220 samples for different times to enable the cultures to achieve the same final cell density (Fig. S4). We
221 quantified the amounts of the control plasmid pHERD30T and the CRISPR-targeted plasmid pCR2SP1
222 present at the beginning of the experiment and we assessed their retention after rapid or slow
223 growth at 37°C to OD_{600} of 1. In spite of CRISPR-targeting of pCR2SP1, after rapid growth, 22% of the
224 plasmids were retained compared to time zero. By contrast, following slow growth, only 0.03% of the
225 plasmids were retained. Thus, CRISPR-Cas interference was > 600-fold more effective during slow
226 growth than during rapid growth (Fig. 4A). Upon extended growth of the rapidly growing culture, the
227 effectiveness of CRISPR-Cas interference increased to levels similar to those of the slowly growing
228 culture (Fig. S5). The pCR2SP1 plasmid carries a protospacer with perfect CRISPR targeting, however it
229 may also prime adaptation, which, in turn, would further increase the frequency of CRISPR targeting
230 and subsequent plasmid curing. In order to address the possibility of priming from the protospacer
231 contributing to the plasmid curing measured in Fig. 4A, we quantified the population-wide level of
232 adaptation at both the beginning and the end of the experiment. Fig. 4B shows that no increase in
233 adaptation frequency occurred during the experiment. Hence, the plasmid curing observed in Fig. 4A
234 can be attributed to CRISPR targeting of the pCR2SP1 plasmid. To determine whether growth rate

235 affects Csy4 levels, we assessed Csy4-3xFLAG amounts following growth at 37° with shaking at 150
236 RPM and 250 RPM to OD_{600} = 1. Fig. 4C shows that growth rate does not affect the abundance of
237 Csy4-3xFLAG.

238

239 **Quorum sensing acts synergistically with temperature to regulate CRISPR-Cas-mediated adaptation.**

240 QS regulates CRISPR-Cas (18, 19). QS relies on the production, release, and group-wide
241 detection of diffusible signaling molecules called autoinducers (AI) and the process allows bacteria to
242 collectively control genes required for group behaviors (34). The major PA14 QS circuit consists of two
243 AI-receptor pairs called LasI/R and RhlI/R. LasI produces the AI 3oxo-C_{12}-homoserine lactone
244 (3OC_{12}HSL), which activates the receptor LasR. LasR activates expression of many genes including
245 those encoding the second QS system, *rhlI/R* (35-38). RhlI synthesizes the AI C_4-homoserine lactone
246 (C_4HSL), that, when bound to RhlR, activates a second wave of QS genes (36).

247 We previously showed that, in PA14, *cas3* expression is activated at high cell density, a
248 hallmark of a QS-regulated trait. Moreover, a PA14 mutant lacking both QS AI synthases, (Δ*lasI* and
249 Δ*rhlI*), exhibited reduced CRISPR-Cas expression, interference, and adaptation compared to WT PA14.
250 Complementation of the Δ*lasI* Δ*rhlI* mutant via exogenous supplementation with the 3OC_{12}HSL and
251 C_4HSL AIs restored CRISPR-Cas function to WT levels (18). We wondered whether the temperature
252 and QS cues function independently or synergistically to regulate CRISPR-Cas. To assess if QS
253 influences temperature-dependent CRISPR adaptation, we used an adaptation assay similar to that
254 shown in Fig. 1. In this case, we assayed CRISPR-Cas-mediated adaptation to the pCR2SP1 seed

255 plasmid in a PA14 Δ*lasI* Δ*rhlI* mutant that lacks the ability to produce the two QS AIs. Colonies were
256 grown in the absence and presence of 2 μM $3OC_{12}HSL$ + 10 μM C_4HSL. Compared to the untreated
257 Δ*lasI* Δ*rhlI* strain, supplementation with AIs increased the frequency of CRISPR adaptation (Fig. 5). The
258 effect of AIs on adaptation frequency was more pronounced at 30°C and 23°C than at 37°C,
259 suggesting that QS and lower temperatures synergistically enhance CRISPR-Cas-mediated adaptation.
260 At 15°C, however, there was no effect of AI supplementation on CRISPR-Cas-directed adaptation
261 frequency, suggesting that at the lowest temperature we tested, temperature alone is sufficient to
262 promote the maximum operating capacity of the CRISPR-Cas system. To examine the role of QS in the
263 temperature-dependent production of Csy4, we measured Csy4-3xFLAG levels in the WT and in the
264 Δ*lasI* Δ*rhlI* strain grown at 37, 30, 23, and 15°C. Because RpoB production is altered in the Δ*lasI* Δ*rhlI*
265 strain relative to WT PA14, we used GroEL as the internal control for this experiment. Fig. S6A shows
266 that, at all temperatures, levels of Csy4-3xFLAG are higher in the WT strain than in the Δ*lasI* Δ*rhlI*
267 strain. Additionally, reducing the temperature promotes increases in Csy4-3xFLAG levels, and this
268 effect is more pronounced in the WT strain than in the Δ*lasI* Δ*rhlI* strain. In agreement with the QS
269 and temperature-dependent findings regarding regulation of Csy4-3xFLAG, interference is more
270 effective in the WT strain than in the Δ*lasI* Δ*rhlI* strain when grown rapidly or slowly (Fig. S6B right
271 panel).

272 Li *et al*. reported that in PA14, CRISPR-Cas degrades *lasR* mRNA, which in turn, affects QS-
273 controlled virulence in a mouse model of infection (39). Therefore, the possibility existed that
274 temperature control of CRISPR-Cas activity could affect LasR receptor levels, resulting in a regulatory
275 feedback loop that contributes to the effects we observe. We could not, however, replicate the

276 findings by Li *et al.* Specifically, qRT-PCR of *lasR* in WT and ΔCRISPR Δ*cas* PA14 showed no differences
277 under any of our experimental conditions (Fig. S7A). We also tested the relative levels of *lasB*,
278 encoding elastase, which is under direct control of LasR (Fig. S7B). Again, there was no effect of
279 CRISPR-Cas on expression of this QS-regulated gene under any condition we tested.

280

281 **Discussion**

282 Here, we discover that temperature is an environmental regulator of CRISPR-Cas interference
283 and adaptation, i.e., target cleavage and acquisition of new immunity spacers, respectively, in *P.*
284 *aeruginosa* PA14. Specifically, CRISPR adaption increases with decreasing temperature. The
285 underlying mechanism appears to rely minimally on increased abundance of CRISPR-Cas components,
286 but rather, primarily on slow growth itself, presumably buying time for the CRISPR-Cas machinery to
287 successfully destroy/adapt to foreign DNA. Given that growth rate and temperature are often
288 connected, this phenomenon could be relevant in other bacteria that harbor CRISPR-Cas systems.

289 *P. aeruginosa* is a soil dwelling organism that is also an opportunistic human pathogen. Phage
290 abundance and diversity are high in ecosystems such as soil, whereas they are particularly limited in
291 the human lung, a major habitat for infectious *P. aeruginosa*, most notably in CF sufferers (24, 25).
292 Our finding that higher CRISPR-Cas activity occurs at lower temperatures correlates with the
293 increased threat of potential foreign parasitic elements in soil (generally at low temperatures)
294 compared to during human infection (generally at 37°C). Thus, we predict that bacteria are better
295 equipped to defend themselves against phage attacks and to adapt to mutating phage in the

296 environment than in the human body, however, one consequence is that bacteria may be vulnerable
297 to higher incidence of autoimmunity in the environment. We recognize that *P. aeruginosa* causes
298 biofilm infections, in which the bacteria exhibit slow growth (40) and that not all *P. aeruginosa*
299 infections in humans are under 37°C conditions. We anticipate that CRISPR-Cas may be more active in
300 *P. aeruginosa* biofilm infections and in superficial wound infections than during bacteremia which
301 would presumably involve planktonic cells at 37°C. Our discovery that low temperatures increase
302 CRISPR adaptation in *P. aeruginosa* suggests that the rarely occurring but crucial naïve adaptation
303 events may take place predominantly during the bacterium's soil dwelling existence and during slow
304 growth in biofilms.

305 Another environmental regulator of CRISPR-Cas in *P. aeruginosa* PA14 is QS. We previously
306 showed that QS, via the two main synthases LasI and RhlI, activates CRISPR-Cas expression,
307 interference, and adaptation (18). Interestingly, in *P. aeruginosa* PAO1, QS is temperature dependent
308 due to the presence of conserved thermo-sensing RNA "thermometers" that reside in the 5'UTRs of
309 *lasI* and *rhlAB-R*, the latter of which controls expression of *rhlR*. Thermoregulation of *lasI* and *rhlR*
310 increases their expression at 37°C compared to 30°C, and consequently, causes increased production
311 of QS-regulated virulence factors (41). Given that, in PAO1, QS regulators and QS-controlled traits are
312 more highly expressed at 37°C than at lower temperatures, one would expect CRISPR-Cas activity to
313 be maximal at 37°C, since we found that QS activates CRISPR-Cas (18). Nonetheless, we do not find
314 this to be the case, at least for PA14. CRISPR-Cas is more active at low temperatures than at high
315 temperatures, and Csy4 is 20-40% more abundant at low temperatures than at high temperatures. To
316 reconcile these findings, we posit that, although the Csy4-3xFLAG protein displays equal stability for

317 up to two hours at 37°C and 23°C, CRISPR-Cas complexes may be more stable at lower temperatures
318 than at higher temperatures, which yields increased levels of assembled CRISPR-Cas complexes, and
319 thus CRISPR-Cas activity, at low temperatures. Additionally, low temperatures may favor more rapid
320 and tighter annealing of crRNA to its target and thereby enhance interference and adaptation.

321 Other reports show correlations between slow growth and CRISPR adaptation. For example, in
322 nutrient poor medium, PA14 primarily acquires CRISPR-based immunity to the phage DMS3^{vir} as
323 opposed to during growth in nutrient rich medium, which, by contrast, promotes accumulation of
324 phage receptor mutations (17). We hypothesize that, under poor growth conditions, increased
325 CRISPR-based adaptation is mediated in part by the slower growth rate of the bacteria compared to
326 that under ideal growth conditions, again, providing the bacteria crucial time to adapt. In the same
327 vein, Amlinger *et al*. discovered that naïve adaptation occurs with the highest frequency in late
328 exponential phase in liquid cultures of *Escherichia coli* overproducing CRISPR-Cas (42). One can
329 imagine that CRISPR-*cas* expression was maintained at a relatively constant level in this experiment
330 due to the use of a synthetic promoter. Thus, maximal adaptation in late exponential phase could be
331 due to the declining growth rate, in agreement with our findings (Fig. 4).

332 Our results showing that slow growth increases the frequency of CRISPR-Cas-mediated
333 plasmid loss suggests that biofilms, which exhibit particularly slow growth in their cores (40, 43), may
334 exhibit exceptionally high CRISPR-Cas activity compared to exponentially growing planktonic cells.
335 High CRISPR-Cas activity in slowly growing cells offers the exciting possibility that transiently growth-
336 arrested antibiotic-tolerant persister subpopulations (44) could be natural reservoirs of cells that are

337 primed for CRISPR adaptation. A phage, upon infecting a persister cell, has its lytic cycle arrested until
338 the host cell resumes growth (45). If CRISPR-Cas is active in persister cells, the persistent stage would
339 afford the host cell ample time for adaptation, possibly providing the cell a means to more efficiently
340 eliminate additional phages that have also infected the cell. Moreover, after resuming growth, the
341 adapted cell would be prepared to fend off infecting phages coming from neighboring cells. Indeed,
342 persistence, which is induced at high cell density when cells are at highest risk of phage infection, may
343 be a form of phage defense. QS increases persister formation in PA14 and PAO1 (46). Thus, QS
344 inhibitors may reduce the fraction of persister cells present, which 1) would allow antibiotics to kill
345 pathogenic bacteria more effectively, and 2) minimize the population of cells that could be
346 particularly prone to acquiring CRISPR-based immunity towards phage therapies. We envision that
347 antibacterial treatments consisting of QS inhibitors, antibiotics, and phage therapies could exhibit
348 exceptional synergy in killing pathogens, including the notorious persister cells. Lastly, and by
349 contrast, our findings offer simple conditions, namely slowing growth rate and/or reducing
350 temperature, that could be explored to increase CRISPR adaptation frequency for applications such as
351 development of phage-resistant bacterial strains, possibly for use in industry or as probiotics.

352

353 **Materials and Methods**

354 **Bacterial strains, plasmids, and phage.** Strains and plasmids used in this study are listed in Table S1.
355 To construct the chromosomal 3x*flag*-tagged *csy4* in PA14, DNA fragments flanking the 3' terminus of
356 *csy4* including a 3x*flag* tag were amplified, sewed together by overlap extension PCR, and cloned into

357 pEXG2 (a generous gift from Joseph Mougous, University of Washington, Seattle) using HindIII and
358 XbaI restriction sites (47). The plasmid to make the ΔCRISPR Δ*cas* PA14 mutant was engineered using
359 the identical strategy and DNA fragments surrounding the CRISPR *cas* locus, flanked by EcoRI and XbaI
360 restriction sites. The resulting plasmids were used to transform *E. coli* SM10*λpir*, and subsequently
361 mobilized into PA14 via mating. Exconjugants were selected on LB (Luria–Bertani) containing
362 gentamicin (30 µg/mL) and irgasan (100 µg/mL), followed by recovery of mutants on M9 medium
363 containing 5% (wt/vol) sucrose. Candidate mutants were confirmed by PCR and sequencing. A PA14
364 strain harboring a CRISPR spacer matching phage JBD44a was generated by cloning 1581 bp of JBD44a
365 gene *gp*33 using native HindIII sites into the adaptation-promoting pCR2SP1 seed plasmid (18). The
366 plasmid was propagated in PA14 on LB agar with 50 µg/mL gentamicin, and single colonies were
367 streaked repeatedly on LB agar and tested for plasmid loss. CRISPR-adapted clones were identified
368 using PCR with primers that enabled assessment of incorporation of spacers into either CRISPR1 or
369 CRISPR2. Newly integrated spacers were identified and mapped using sequencing. A strain with the
370 new spacer AGCCACAACANAGGCCAGAGAAGCTGCTGCGA in CRISPR2 that targeted gene *gp33* was
371 selected and tested for resistance to JBD44a by a cross streak assay. Primers are listed in
372 Supplementary Table S2.

373 **Growth Conditions.** PA14 and mutants were grown at the indicated temperatures in LB broth or on
374 LB solidified with 15 g agar/L. LB was supplemented with 50 µg/mL gentamicin where appropriate. For
375 AI supplementation assays, $3OC_{12}HSL$ and C_4HSL (Sigma), or the solvent DMSO was used. Growth of
376 bacterial cultures was measured by OD_{600}, where 1 unit = 10^9 CFU/mL.

377 **Adaptation Assay.** WT PA14 and the Δ*lasI* Δ*rhlI* mutant were transformed with pCR2SP1 seed as
378 described previously (18) and plated on LB medium containing 50 µg/mL gentamicin and, in the case
379 of the Δ*lasI* Δ*rhlI* mutant, either DMSO (control) or 2 µM $3OC_{12}HSL$ + 10 µM C_4HSL (designated AI) was
380 added. The plates were incubated at 37, 30, 23, and 15°C until the colonies were 1 mm in diameter.
381 Single colonies were tested for population-wide integration of new CRISPR spacers against the
382 CRISPR-targeted plasmid by PCR using DreamTaq Green PCR Master Mix (Thermo Fisher) with primers
383 designed to anneal upstream of the CRISPR2 array and inside the second spacer, which enabled
384 detection of expansion of this array. The PCR products were subjected to agarose gel electrophoresis
385 and band intensities were analyzed using Image Quant TL software (GE Healthcare).

386 **Relative plasmid copy number.** PA14 harboring pHERD30T, the empty vector backbone for the
387 pCR2SP1 seed plasmid, was grown at 37, 30, 23, and 15°C on LB agar supplemented with gentamicin
388 (50 µg/mL). Total DNA was extracted from individual colonies that were 1 mm in size using DNeasy
389 Blood & Tissue Kit (Qiagen). qPCR was performed using PerfeCTa® SYBR® Green FastMix®, Low ROX
390 ($Quanta^{bio}$) with primers specific for pHERD30T and chromosomal *rpoB*.

391 **Western blot.** The PA14 *csy4*-3x*flag* and Δ*lasI* Δ*rhlI csy4*-3x*flag* strains were streaked onto LB medium
392 and grown at 37, 30, 23, or 15°C until individual colonies reached 1 mm in diameter. Single colonies
393 were harvested and lysed with BugBuster protein extraction regent (Millipore), following the
394 manufacturer's instructions. 50 µg protein was separated by SDS-PAGE on a 4–20% Mini-PROTEAN®
395 TGX™ polyacrylamide gel (Bio-Rad) and blotted onto a PVDF membrane (1620174, Bio-Rad). The
396 membrane was incubated for 1 h with monoclonal ANTI-FLAG® M2-Peroxidase (HRP) antibody

397 (A8592, SIGMA), monoclonal anti-RpoB antibody (Abcam, ab191598), both at 1:3,000, or polyclonal
398 anti-GroEL antibody (G6532, SIGMA) at 1:15,000 in TBST and 5% skim milk. Anti-rabbit antibody
399 (Promega, W4011) was used as the secondary antibody for detection of the anti-RpoB and anti-GroEL
400 antibodies. The membrane was washed in TBST and was developed using SuperSignal West Femto
401 Maximum Sensitivity Substrate (34095, Thermo Scientific).

402

403 **Acknowledgements**

404 We thank Dr. Jon E. Paczkowski and other members of the B.L.B. group for helpful suggestions. We
405 thank Dr. George O'Toole, Dr. Joseph Mougous, and Dr. Joseph Bondy-Denomy for providing bacterial
406 strains and phage. This work was supported by the Howard Hughes Medical Institute, NIH Grant
407 2R37GM065859, and National Science Foundation Grant MCB-1713731 (to B.L.B.); an Alexander von
408 Humboldt-Max Planck Society Award, the Danish Council for Independent Research Postdoctoral
409 Fellowship DFF-4090-00265, administered by the University of Copenhagen, and a Lundbeck
410 Fellowship R220-2016-860 (to N.M.H.-K.).

411

412 **References**

413 1. Barrangou R, Fremaux C, Deveau H, Richards M, Boyaval P, Moineau S, Romero DA, Horvath P.
414 2007. CRISPR provides acquired resistance against viruses in prokaryotes. Science 315:1709-
415 12.

416 2. Marraffini LA, Sontheimer EJ. 2008. CRISPR interference limits horizontal gene transfer in
417 staphylococci by targeting DNA. Science 322:1843-5.
418 3. Marraffini LA. 2015. CRISPR-Cas immunity in prokaryotes. Nature 526:55-61.
419 4. Nunez JK, Lee AS, Engelman A, Doudna JA. 2015. Integrase-mediated spacer acquisition during
420 CRISPR-Cas adaptive immunity. Nature 519:193-8.
421 5. Datsenko KA, Pougach K, Tikhonov A, Wanner BL, Severinov K, Semenova E. 2012. Molecular
422 memory of prior infections activates the CRISPR/Cas adaptive bacterial immunity system. Nat
423 Commun 3:945.
424 6. Brouns SJ, Jore MM, Lundgren M, Westra ER, Slijkhuis RJ, Snijders AP, Dickman MJ, Makarova
425 KS, Koonin EV, van der Oost J. 2008. Small CRISPR RNAs guide antiviral defense in prokaryotes.
426 Science 321:960-4.
427 7. Mojica FJ, Diez-Villasenor C, Garcia-Martinez J, Almendros C. 2009. Short motif sequences
428 determine the targets of the prokaryotic CRISPR defence system. Microbiology 155:733-40.
429 8. Westra ER, Semenova E, Datsenko KA, Jackson RN, Wiedenheft B, Severinov K, Brouns SJ.
430 2013. Type I-E CRISPR-cas systems discriminate target from non-target DNA through base
431 pairing-independent PAM recognition. PLoS Genet 9:e1003742.
432 9. Garneau JE, Dupuis ME, Villion M, Romero DA, Barrangou R, Boyaval P, Fremaux C, Horvath P,
433 Magadan AH, Moineau S. 2010. The CRISPR/Cas bacterial immune system cleaves
434 bacteriophage and plasmid DNA. Nature 468:67-71.
435 10. McGinn J, Marraffini LA. 2018. Molecular mechanisms of CRISPR-Cas spacer acquisition. Nat
436 Rev Microbiol doi:10.1038/s41579-018-0071-7.

437 11. Staals RH, Jackson SA, Biswas A, Brouns SJ, Brown CM, Fineran PC. 2016. Interference-driven
438 spacer acquisition is dominant over naive and primed adaptation in a native CRISPR-Cas
439 system. Nat Commun 7:12853.
440 12. van Houte S, Ekroth AK, Broniewski JM, Chabas H, Ben A, Bondy-Denomy J, Gandon S, Boots
441 M, Paterson S, Buckling A, Westra ER. 2016. The diversity-generating benefits of a prokaryotic
442 adaptive immune system. Nature doi:10.1038/nature17436.
443 13. Hynes AP, Villion M, Moineau S. 2014. Adaptation in bacterial CRISPR-Cas immunity can be
444 driven by defective phages. Nat Commun 5:4399.
445 14. Agari Y, Sakamoto K, Tamakoshi M, Oshima T, Kuramitsu S, Shinkai A. 2010. Transcription
446 profile of Thermus thermophilus CRISPR systems after phage infection. J Mol Biol 395:270-81.
447 15. Patterson AG, Chang JT, Taylor C, Fineran PC. 2015. Regulation of the Type I-F CRISPR-Cas
448 system by CRP-cAMP and GalM controls spacer acquisition and interference. Nucleic Acids Res
449 43:6038-48.
450 16. Yang CD, Chen YH, Huang HY, Huang HD, Tseng CP. 2014. CRP represses the CRISPR/Cas
451 system in Escherichia coli: evidence that endogenous CRISPR spacers impede phage P1
452 replication. Mol Microbiol 92:1072-91.
453 17. Westra ER, van Houte S, Oyesiku-Blakemore S, Makin B, Broniewski JM, Best A, Bondy-
454 Denomy J, Davidson A, Boots M, Buckling A. 2015. Parasite Exposure Drives Selective Evolution
455 of Constitutive versus Inducible Defense. Curr Biol 25:1043-9.

456 18. Hoyland-Kroghsbo NM, Paczkowski J, Mukherjee S, Broniewski J, Westra E, Bondy-Denomy J,
457 Bassler BL. 2017. Quorum sensing controls the Pseudomonas aeruginosa CRISPR-Cas adaptive
458 immune system. Proc Natl Acad Sci U S A 114:131-135.
459 19. Patterson AG, Jackson SA, Taylor C, Evans GB, Salmond GPC, Przybilski R, Staals RHJ, Fineran
460 PC. 2016. Quorum Sensing Controls Adaptive Immunity through the Regulation of Multiple
461 CRISPR-Cas Systems. Mol Cell 64:1102-1108.
462 20. Rybtke M, Hultqvist LD, Givskov M, Tolker-Nielsen T. 2015. Pseudomonas aeruginosa Biofilm
463 Infections: Community Structure, Antimicrobial Tolerance and Immune Response. J Mol Biol
464 427:3628-45.
465 21. Rahme LG, Stevens EJ, Wolfort SF, Shao J, Tompkins RG, Ausubel FM. 1995. Common virulence
466 factors for bacterial pathogenicity in plants and animals. Science 268:1899-902.
467 22. Wiedenheft B, van Duijn E, Bultema JB, Waghmare SP, Zhou K, Barendregt A, Westphal W,
468 Heck AJ, Boekema EJ, Dickman MJ, Doudna JA. 2011. RNA-guided complex from a bacterial
469 immune system enhances target recognition through seed sequence interactions. Proc Natl
470 Acad Sci U S A 108:10092-7.
471 23. Cady KC, Bondy-Denomy J, Heussler GE, Davidson AR, O'Toole GA. 2012. The CRISPR/Cas
472 adaptive immune system of Pseudomonas aeruginosa mediates resistance to naturally
473 occurring and engineered phages. J Bacteriol 194:5728-38.
474 24. Aziz RK, Dwivedi B, Akhter S, Breitbart M, Edwards RA. 2015. Multidimensional metrics for
475 estimating phage abundance, distribution, gene density, and sequence coverage in
476 metagenomes. Front Microbiol 6:381.

477 25. Willner D, Furlan M, Haynes M, Schmieder R, Angly FE, Silva J, Tammadoni S, Nosrat B, Conrad
478 D, Rohwer F. 2009. Metagenomic analysis of respiratory tract DNA viral communities in cystic
479 fibrosis and non-cystic fibrosis individuals. PLoS One 4:e7370.
480 26. Li M, Wang R, Xiang H. 2014. Haloarcula hispanica CRISPR authenticates PAM of a target
481 sequence to prime discriminative adaptation. Nucleic Acids Res 42:7226-35.
482 27. Shan J, Korbsrisate S, Withatanung P, Adler NL, Clokie MR, Galyov EE. 2014. Temperature
483 dependent bacteriophages of a tropical bacterial pathogen. Front Microbiol 5:599.
484 28. Chu TC, Murray SR, Hsu SF, Vega Q, Lee LH. 2011. Temperature-induced activation of
485 freshwater Cyanophage AS-1 prophage. Acta Histochem 113:294-9.
486 29. Sanders ME, Klaenhammer TR. 1984. Phage Resistance in a Phage-Insensitive Strain of
487 Streptococcus lactis: Temperature-Dependent Phage Development and Host-Controlled Phage
488 Replication. Appl Environ Microbiol 47:979-85.
489 30. O'Driscoll J, Glynn F, Cahalane O, O'Connell-Motherway M, Fitzgerald GF, Van Sinderen D.
490 2004. Lactococcal plasmid pNP40 encodes a novel, temperature-sensitive restriction-
491 modification system. Appl Environ Microbiol 70:5546-56.
492 31. Kropinski AM, Lewis V, Berry D. 1987. Effect of growth temperature on the lipids, outer
493 membrane proteins, and lipopolysaccharides of Pseudomonas aeruginosa PAO. J Bacteriol
494 169:1960-6.
495 32. McGroarty EJ, Rivera M. 1990. Growth-dependent alterations in production of serotype-
496 specific and common antigen lipopolysaccharides in Pseudomonas aeruginosa PAO1. Infect
497 Immun 58:1030-7.

498 33. Shinkai A, Kira S, Nakagawa N, Kashihara A, Kuramitsu S, Yokoyama S. 2007. Transcription
499 activation mediated by a cyclic AMP receptor protein from Thermus thermophilus HB8. J
500 Bacteriol 189:3891-901.
501 34. Papenfort K, Bassler BL. 2016. Quorum sensing signal-response systems in Gram-negative
502 bacteria. Nat Rev Microbiol 14:576-88.
503 35. Pesci EC, Pearson JP, Seed PC, Iglewski BH. 1997. Regulation of las and rhl quorum sensing in
504 Pseudomonas aeruginosa. J Bacteriol 179:3127-32.
505 36. Pearson JP, Passador L, Iglewski BH, Greenberg EP. 1995. A second N-acylhomoserine lactone
506 signal produced by Pseudomonas aeruginosa. Proc Natl Acad Sci U S A 92:1490-4.
507 37. Gambello MJ, Kaye S, Iglewski BH. 1993. LasR of Pseudomonas aeruginosa is a transcriptional
508 activator of the alkaline protease gene (apr) and an enhancer of exotoxin A expression.
509 Infection and immunity 61:1180-4.
510 38. Seed PC, Passador L, Iglewski BH. 1995. Activation of the Pseudomonas aeruginosa lasI gene by
511 LasR and the Pseudomonas autoinducer PAI: an autoinduction regulatory hierarchy. Journal of
512 bacteriology 177:654-9.
513 39. Li R, Fang L, Tan S, Yu M, Li X, He S, Wei Y, Li G, Jiang J, Wu M. 2016. Type I CRISPR-Cas targets
514 endogenous genes and regulates virulence to evade mammalian host immunity. Cell Res
515 26:1273-1287.
516 40. Werner E, Roe F, Bugnicourt A, Franklin MJ, Heydorn A, Molin S, Pitts B, Stewart PS. 2004.
517 Stratified growth in Pseudomonas aeruginosa biofilms. Appl Environ Microbiol 70:6188-96.

518 41. Grosso-Becerra MV, Croda-Garcia G, Merino E, Servin-Gonzalez L, Mojica-Espinosa R, Soberon-
519 Chavez G. 2014. Regulation of Pseudomonas aeruginosa virulence factors by two novel RNA
520 thermometers. Proc Natl Acad Sci U S A 111:15562-7.
521 42. Amlinger L, Hoekzema M, Wagner EGH, Koskiniemi S, Lundgren M. 2017. Fluorescent CRISPR
522 Adaptation Reporter for rapid quantification of spacer acquisition. Sci Rep 7:10392.
523 43. Wentland EJ, Stewart PS, Huang CT, McFeters GA. 1996. Spatial variations in growth rate
524 within Klebsiella pneumoniae colonies and biofilm. Biotechnol Prog 12:316-21.
525 44. Harms A, Maisonneuve E, Gerdes K. 2016. Mechanisms of bacterial persistence during stress
526 and antibiotic exposure. Science 354.
527 45. Pearl S, Gabay C, Kishony R, Oppenheim A, Balaban NQ. 2008. Nongenetic individuality in the
528 host-phage interaction. PLoS Biol 6:e120.
529 46. Moker N, Dean CR, Tao J. 2010. Pseudomonas aeruginosa increases formation of multidrug-
530 tolerant persister cells in response to quorum-sensing signaling molecules. J Bacteriol
531 192:1946-55.
532 47. Rietsch A, Vallet-Gely I, Dove SL, Mekalanos JJ. 2005. ExsE, a secreted regulator of type III
533 secretion genes in Pseudomonas aeruginosa. Proc Natl Acad Sci U S A 102:8006-11.

534

535 **Figure 1. CRISPR adaptation is temperature dependent.**

536 Integration of new CRISPR spacers into the CRISPR2 locus was measured by PCR amplification of the
537 CRISPR2 array region from single colonies of PA14 and the Δ*cas3* mutant. Both strains harbored the

538 CRISPR-targeted plasmid, pCR2SP1 seed, containing a seed mutation that promotes adaptation. Each
539 adaptation event results in acquisition of a new spacer (32 bp) and CRISPR repeat (28 bp), which is
540 exhibited by a 60 bp increase in size of the CRISPR locus, and can be visualized by gel electrophoresis.
541 (A) Adaptation of PA14 cells carrying pCR2SP1 seed at 37, 30, 23, or 15°C. The Δ*cas3* mutant is
542 incapable of cleaving DNA bound by the Csy1-4 complex and serves as a negative control for
543 adaptation. Data are shown for representative colonies. (B) Quantitation of the spacer population in
544 (A), n = 6.

545

546 **Figure 2. Temperature does not affect the relative copy number of pHERD30T in PA14.**

547 PA14 harboring pHERD30T, the empty vector backbone for the pCR2SP1 seed plasmid, was grown at
548 37, 30, 23, and 15°C on LB agar supplemented with gentamicin (50 µg/mL). The copy number of
549 plasmid DNA relative to chromosomal DNA was measured by qPCR of total DNA using primers for
550 pHERD30T and *rpoB*. Error bars represent SD from n = 3 replicates (P = 0.1752. One-way ANOVA
551 analysis).

552

553 **Figure 3. Csy4 levels are modestly upregulated at low temperatures.**

554 Western blot of PA14 Csy4-3xFLAG grown at 37, 30, 23, and 15°C. The upper panel shows the
555 abundance of RpoB which was used as the endogenous control. The lower panel shows the

556 abundance of Csy4-3xFLAG. Quantitation of the relative abundance of Csy4-3xFLAG normalized to
557 RpoB is shown below the blot. The data are representative of > 3 independent experiments.

558

559 **Figure 4. Growth rate affects CRISPR-Cas activity.**

560 (A) Retention of the control parent plasmid pHERD30T (black) and the CRISPR-targeted plasmid
561 pCR2SP1 (gray) in PA14 grown at 37°C to OD_{600} = 1 with aeration at 250 RPM (denoted rapid growth)
562 or 150 RPM (denoted slow growth). 100% denotes no plasmid loss. SD represents 3 replicates. ($P <$
563 0.0001. Student's *t*-test). (B) Adaptation of PA14 cells carrying pCR2SP1 grown as in (A), at T = 0 and at
564 the end of the experiment, at OD_{600} = 1. (C) Western blot of PA14 Csy4-3xFLAG grown as in (A) to
565 OD_{600} = 1. The upper panel shows the abundance of RpoB which was used as the endogenous control.
566 The lower panel shows the abundance of Csy4-3xFLAG. Quantitation of the relative abundance of
567 Csy4-3xFLAG normalized to RpoB is shown below the blot.

568

569 **Figure 5. QS and low temperature act synergistically to enhance CRISPR-Cas-mediated adaptation.**

570 PCR amplification of the CRISPR2 array and visualization by gel electrophoresis, as in Fig. 1. The PA14
571 Δ*lasI* Δ*rhlI* mutant does not produce $3OC_{12}HSL$ or C_4HSL. $3OC_{12}HSL$ and C_4HSL (designated AI) were
572 supplied at saturating concentrations (2 µM and 10 µM, respectively) as denoted. The data are
573 representative of > 3 independent experiments.

574

575 **Supplemental Material**

576

577 **Supplementary Table S1. Bacterial strains, phage, and plasmids.**

578 **Supplementary Table S2. Primers used in this study.**

579 **Supplementary Figure S1. The 3xFLAG tagged Csy4 protein is functional.**

580 WT PA14, *csy4*-3x*flag*, and ΔCRISPR Δ*cas* strains were streaked (left to right) across the virulent phage
581 DMS3m^{vir} (indicated by the vertical dotted line). DMS3m^{vir} is targeted by PA14 CRISPR2 spacer 1. A
582 functional CRISPR-Cas apparatus protects PA14 cells against this phage (23).

583

584 **Supplementary Figure S2. Csy4-3xFLAG stability at 37°C and 23°C.**

585 Western blot of PA14 Csy4-3xFLAG. Cultures were grown to OD_{600} = 1 at 23°C, gentamicin was added
586 to arrest protein synthesis, the cultures were divided into two aliquots, and one was incubated at
587 37°C and the other at 23°C. Samples were taken at 0, 30, 60, and 120 min after addition of
588 gentamicin. The upper panel shows the abundance of RpoB which was used as the endogenous
589 control. The lower panel shows the abundance of Csy4-3xFLAG.

590

591 **Supplementary Figure S3. Temperature affects phage adsorption independently of CRISPR-Cas.**

592 WT PA14, a ΔCRISPR Δ*cas* mutant, and a WT^R strain carrying a CRISPR spacer targeting JBD44a, were
593 grown to OD_{600} = 1 at 37°C (A) or 23°C (B) and infected with phage JBD44a at an MOI of 30. PFU were
594 quantified over time. SD represents 3 replicates. Cells grown at 23°C adsorb phage at a higher rate
595 than those grown at 37°C.

596

597 **Supplementary Figure S4. Growth curves for PA14 grown at 150 (Slow) and 250 (Rapid) RPM.**

598 Colonies of PA14 carrying the pHERD30T plasmid were inoculated in LB broth and grown at 37°C with
599 rapid (250 RPM) or slow (150 RPM) shaking. Growth was measured as OD_{600}. The doubling time of
600 PA14 during rapid exponential growth is 32.6 min (R^2 = 0.9996). During slow exponential growth,
601 between OD_{600} 0.025 - 0.2, the doubling time is 61.4 min (R^2 = 0.9791), and between OD_{600} 0.2 and
602 0.7, the doubling time is 185.3 min (R^2 = 0.9546). n = 3.

603

604 **Supplementary Figure S5. Plasmid loss after extended growth.**

605 The data in this figure extend the analyses shown in Fig. 4A. In Fig. 4A, cultures of PA14 carrying
606 pCR2SP1 were grown at 37°C with shaking at 150 RPM (slow growth) or 250 RPM (rapid growth) until
607 each culture reached OD_{600} = 1. Here, we show data for cultures grown at 250 RPM for an extended
608 time; a time equal to that required for the cultures grown at 150 RPM to reach OD_{600} = 1. The data
609 show that increased growth time at 250 RPM, which enables the culture to enter stationary phase,

610 causes increased loss of both the untargeted pHERD30T plasmid and the CRISPR-targeted pCR2SP1
611 plasmid.

612

613 **Supplementary Figure S6. The effect of QS on temperature-dependent Csy4 regulation and growth**
614 **rate regulation of CRISPR-Cas activity.**

615 (A) Western blot of PA14 Csy4-3xFLAG grown at 37, 30, 23, and 15°C. The upper panel shows the
616 abundance of GroEL which was used as the endogenous control. The lower panel shows the
617 abundance of Csy4-3xFLAG. Quantitation of the relative abundance of Csy4-3xFLAG normalized to
618 GroEL is shown below the blot. (B) Retention of the control parent plasmid pHERD30T (left panel) and
619 the CRISPR-targeted plasmid pCR2SP1 (right panel) in WT PA14 and the Δ*lasI* Δ*rhlI* strain grown at
620 37°C to OD_{600} = 1 with aeration at 250 RPM (denoted rapid growth) or 150 RPM (denoted slow
621 growth). 100% denotes no plasmid loss. SD represents 3 replicates. ($P < 0.001$ for pCR2SP1. Student's
622 *t*-test).

623

624 **Supplementary Figure S7. CRISPR-Cas does not regulate *lasR* or *lasB*.**

625 (A) Relative *lasR* mRNA levels normalized to 5S RNA were measured by qRT-PCR in PA14 and in the
626 isogenic ΔCRISPR Δ*cas* strain under different QS states (OD_{600} = 1 and 2). (B) As in panel A, showing
627 *lasB* mRNA, encoding the virulence factor elastase, transcription of which is activated by LasR. Error
628 bars represent SD from n = 3 replicates. ($P > 0.05$. Student's t-test). Unlike the results obtained by Li *et*

629 *al*. (39), under our experimental conditions, CRISPR-Cas neither affects the relative levels of *lasR*

630 mRNA nor LasR-regulated *lasB* mRNA levels.

Fig. 1 A

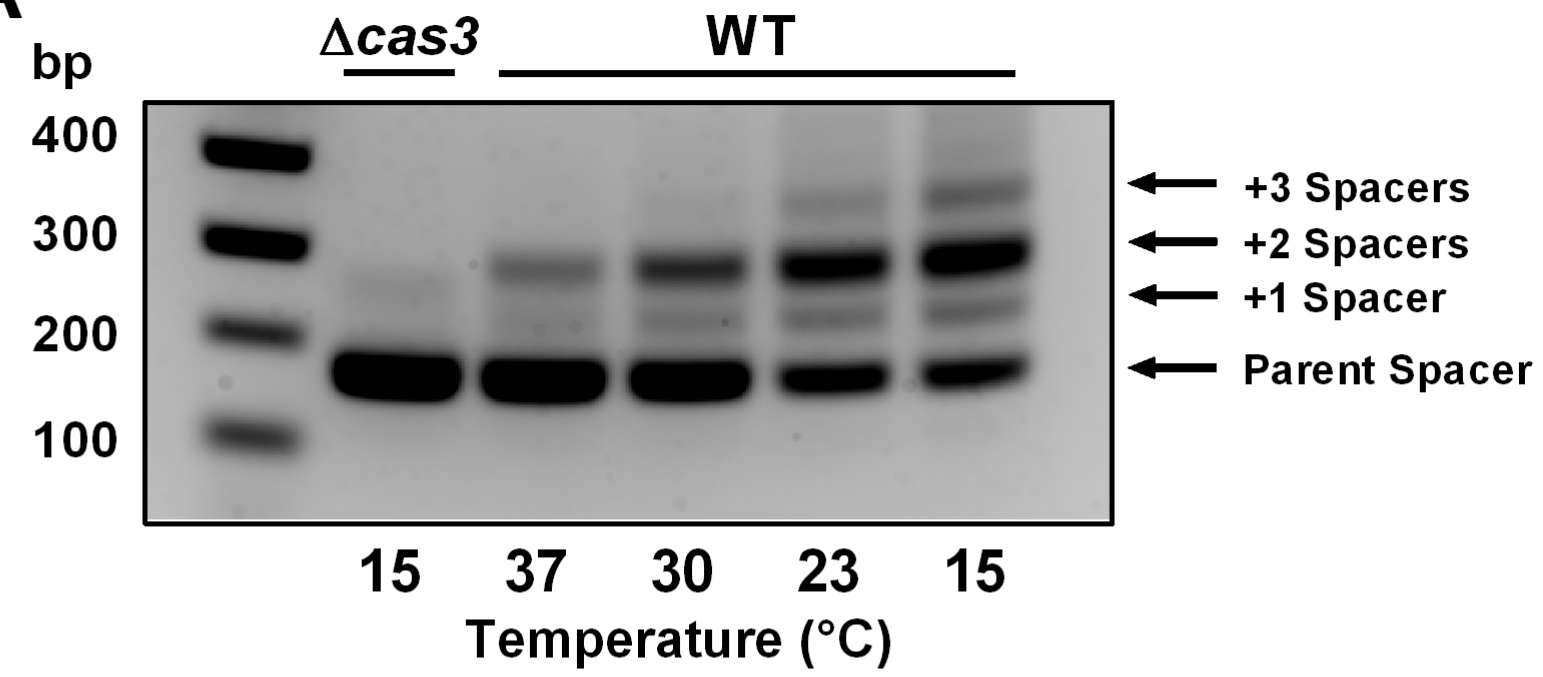
bp
Δcas3
WT
400
300
200
100
+3 Spacers
+2 Spacers
+1 Spacer
Parent Spacer
15
37
30
23
15
Temperature (°C)

B

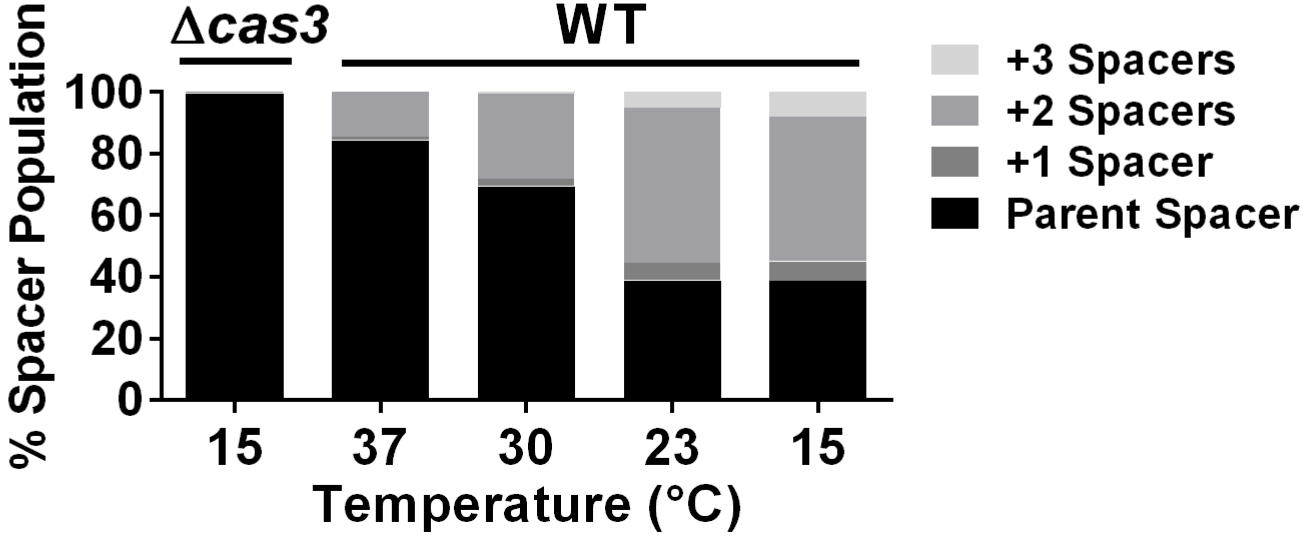
Δcas3
WT
% Spacer Population
100
80
60
40
20
0
+3 Spacers
+2 Spacers
+1 Spacer
Parent Spacer
15
37
30
23
15
Temperature (°C)

Fig. 2

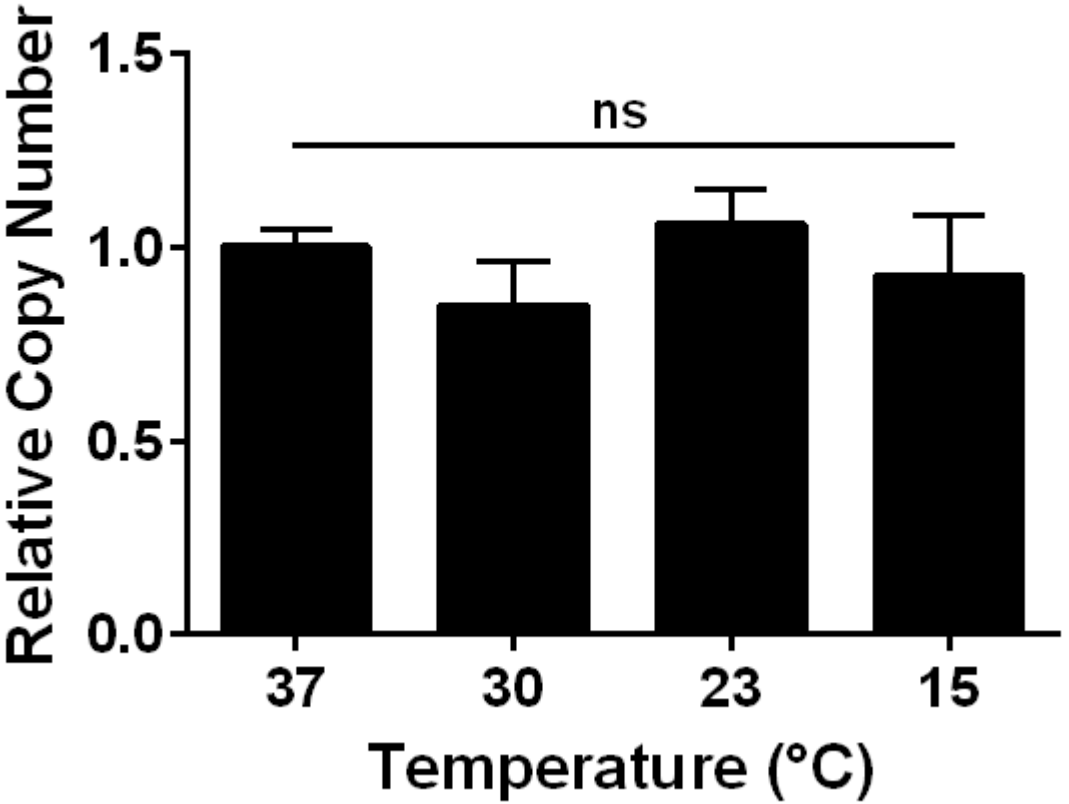

Fig. 3

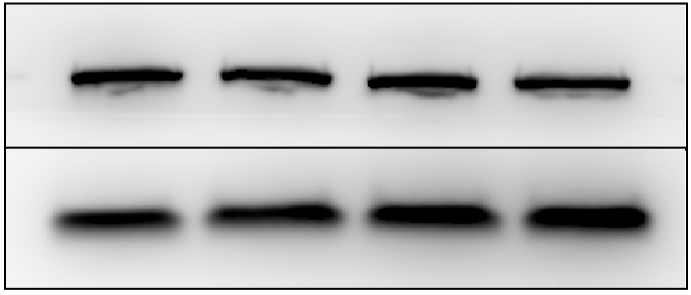

Fig. 4

A

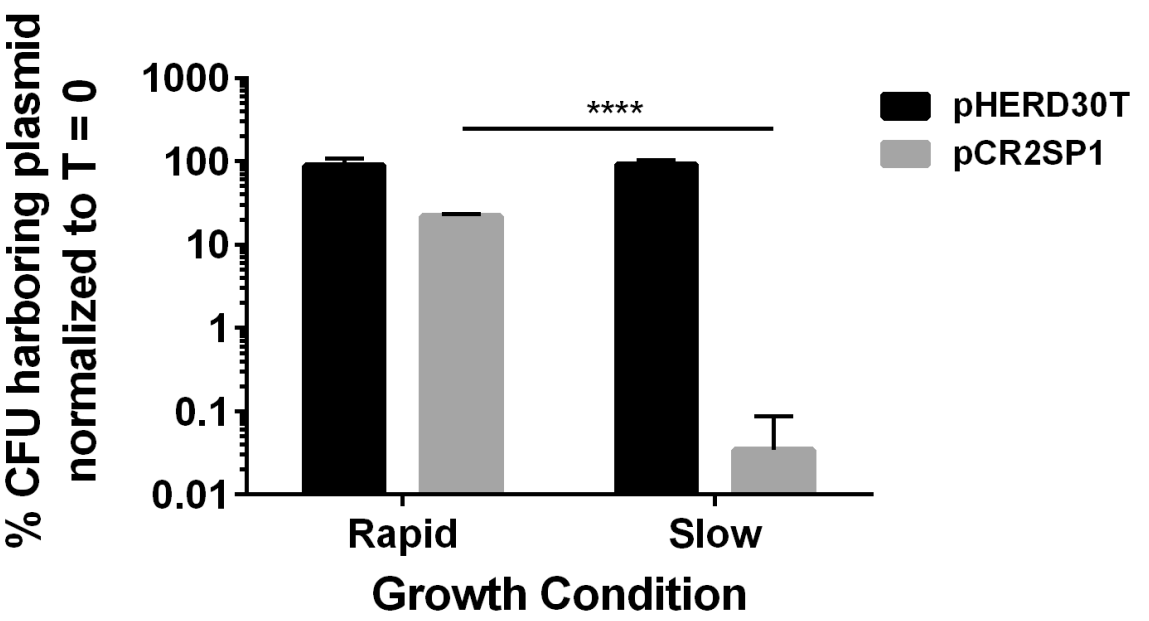
% CFU harboring plasmid normalized to T = 0
1000
100
10
1
0.1
0.01
****
pHERD30T
pCR2SP1
Rapid
Slow
Growth Condition

B

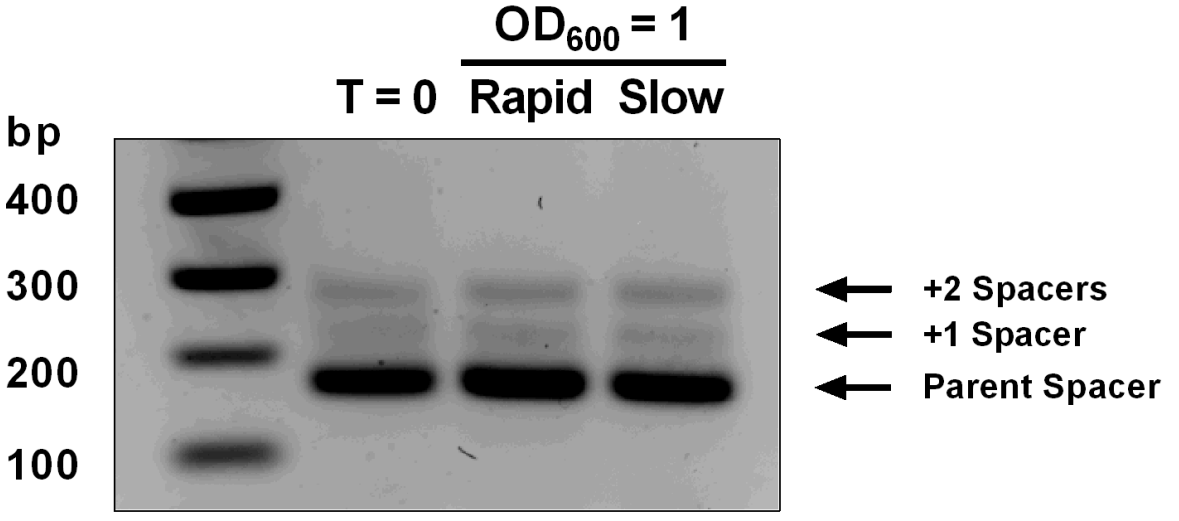
OD600 = 1
T = 0
Rapid
Slow
bp
400
300
200
100
+2 Spacers
+1 Spacer
Parent Spacer

C

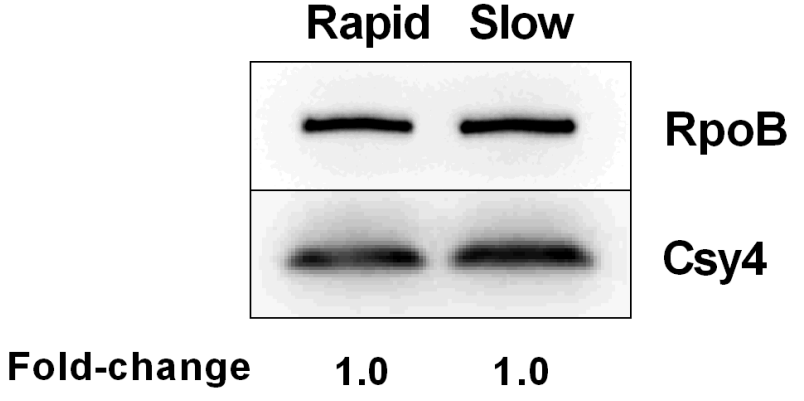
Rapid
Slow
RpoB
Csy4
Fold-change
1.0
1.0

Fig. 5

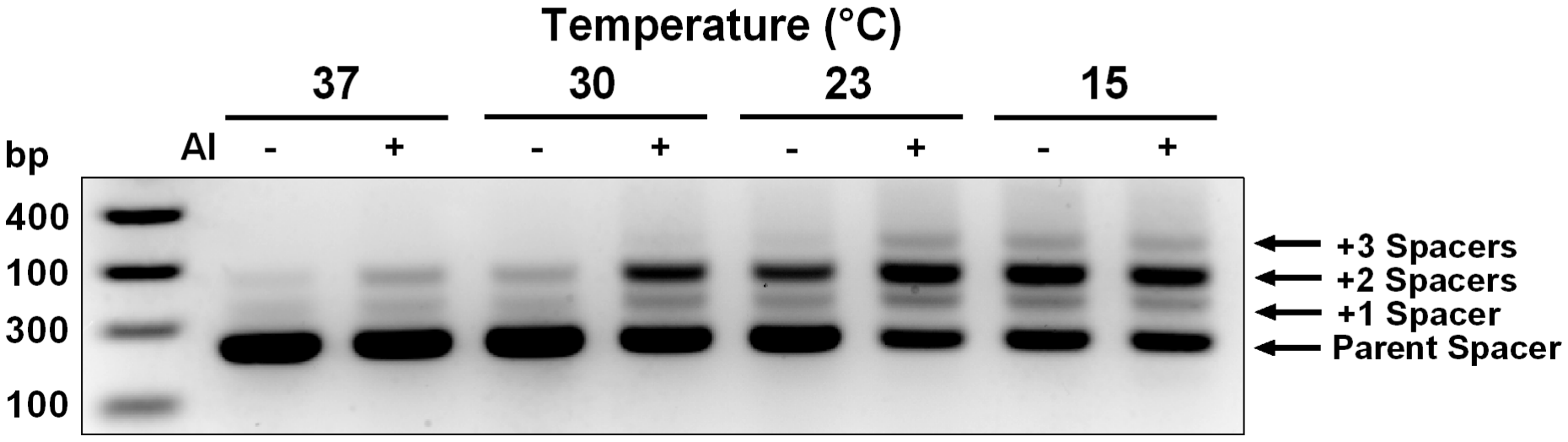
Temperature (°C)
37
30
23
15
bp
AI
-
+
-
+
-
+
-
+
400
100
300
100
+3 Spacers
+2 Spacers
+1 Spacer
Parent Spacer